sp-band tight-binding model for the Bychkov-Rashba effect in a two-dimensional electron system including nearest-neighbor contributions from an electric field

Christian R. Ast* and Isabella Gierz
Max-Planck-Institut für Festkörperforschung, 70569 Stuttgart, Germany
(Received 25 January 2012; published 2 August 2012)

We present a tight-binding calculation for a two-dimensional electron gas (2DEG) including the spin-orbit interaction as well as an electric field perpendicular to the system in order to model the Bychkov-Rashba spin splitting. The associated potential gradient introduces two contributions to the tight-binding matrix: an on-site contribution coupling orbitals of the same atom and a nearest-neighbor contribution. At the $\overline{\Gamma}$ point the first-order Rashba constant α_R only depends on this nearest-neighbor contribution regardless of the lattices considered (square, hexagonal, honeycomb). Applying the model to graphene reveals that this nearest-neighbor contribution induces a significant increase in the zeroth-order Rashba constant λ_R and introduces a spin-splitting component, which varies linearly in momentum.

DOI: 10.1103/PhysRevB.86.085105 PACS number(s): 73.20.−r, 73.22.Pr

I. INTRODUCTION

The Bychkov-Rashba (BR) model has been remarkably successful in qualitatively describing the lifting of the spin degeneracy in a two-dimensional (2D) electron gas by means of a perpendicular electric field.[1] However, it is a phenomenological model that does not include the atomic spin-orbit interaction or any details about the potential landscape of the crystal lattice. Therefore the electric field that enters the first-order Rashba constant α_R has to be regarded as an effective field whose magnitude cannot be predicted based on the BR model. Petersen and Hedegård have related the first-order Rashba coupling constant α_R to the parameters of a simple p-band tight-binding model including spin-orbit coupling which enabled them to make quantitative predictions for the size of the spin splitting.[2] In their model, the atomic spin-orbit coupling enters through the $\mathbf{L}\cdot\mathbf{S}$ Hamiltonian and the potential gradient results in a nonzero overlap of the in-plane p_x and p_y orbitals with the out-of-plane p_z orbital of a neighboring atom. The first-order Rashba constant α_R then depends on the atomic spin-orbit coupling parameter α as well as a parameter γ accounting for the influence of the potential gradient perpendicular to the 2D system. This potential gradient may also be interpreted in terms of an effective potential resulting from an asymmetric hybridization of orbitals at the surface.

Recently, the tight-binding approach has also been used to describe the Rashba-type spin splitting in graphene.[3–6] Here as well, the effective spin-orbit coupling parameter Δ_{SO} as well as the zeroth-order Rashba parameter λ_R accounting for an electric field perpendicular to the graphene plane have been expressed analytically in terms of the tight-binding parameters. Konschuh *et al.*[4] also considered contributions from d orbitals, but they did not directly consider the nearest-neighbor contribution from the electric field. For graphene, so far, the nearest-neighbor contribution of the electric field has only been considered phenomenologically.[6] This phenomenological model has already been successfully applied to honeycomb lattices as well as the Au(111) surface.[7–9] A contribution from the electric field is expected from a coupling of orbitals in neighboring atoms as already indicated by Petersen and Hedegård[2] yielding the same effective Hamiltonian as the phenomenological model.[6,8] The question arises how the different on-site and nearest-neighbor contributions can be unified on common grounds.

Here, we present a generalization of the sp-band tight-binding models used for graphene[3–5] as well as the one presented by Petersen and Hedegård.[2] We calculate the effect of a constant potential gradient ξ in the direction perpendicular to the 2D electron system (z direction) separated into a contribution from the orbitals within the same atom as well as a contribution from orbitals of neighboring atoms. While the on-site contribution couples orbitals according to the well-known dipole selection rules $\Delta l = \pm 1$ and $\Delta m = 0$, the contribution from neighboring atoms also couples orbitals with $\Delta l = 0$ and $\Delta m \neq 0$. We will discuss the findings for the model system graphene, where additional interesting contributions to the Rashba parameter emerge. Finally, we apply this model to the band structure at the $\overline{\Gamma}$ point in different two-dimensional lattices.

II. TIGHT-BINDING MODEL

The Hamiltonian that we employ can be divided into three different contributions:

$$H = H^{\mathrm{tb}} + H^{\mathrm{SOC}} + H^{z}. \tag{1}$$

The first term is the tight-binding Hamiltonian describing the band structure in the linear combination of atomic orbitals (LCAO) approximation.[10] Here, we will only consider s and p orbitals with on-site contributions ϵ_s and ϵ_p, respectively. The tight-binding parameters describing the orbital overlap from neighboring atoms are $V_{ss\sigma}$, $V_{sp\sigma}$, $V_{pp\sigma}$, and $V_{pp\pi}$. The corresponding matrix is then

$$H^{\mathrm{tb}}_{o,o'} = \epsilon_o \delta_{o,o'} + \sum_{\langle i\rangle} e^{i\mathbf{k}\mathbf{R}_i} E(o,o',\mathbf{R}_i). \tag{2}$$

Here, o and o' are the orbitals (s, p_x, p_y, p_z) in the tight-binding matrix and $\delta_{o,o'}$ is the Kronecker δ. In the second term of Eq. (2), $E(o,o',\mathbf{R}_i) = \langle o|H^{\mathrm{tb}}|o',\mathbf{R}_i\rangle$ is an element from Table I. $\langle i\rangle$ denotes the sum over neighboring atoms with $\mathbf{R}_i$ being the vector connecting two neighboring atoms. If there

TABLE I. Matrix elements for the s and p orbitals (Ref. 10). Values that are not given can be obtained by cyclic permutation. The quantities u, v, and w, which depend on the vector $\mathbf{R}_i$ connecting two neighboring atoms, are the directional cosines in the x, y, and z direction, respectively. It should be noted that matrix elements with same (different) parity between orbitals transform even (odd) under exchange of indices $[E(o',o,-\mathbf{R}_i) = (-1)^{|l-l'|}E(o,o',\mathbf{R}_i)]$.

Parameter	Overlap
$E(s,s,\mathbf{R}_i)$	$V_{ss\sigma}$
$E(s,p_x,\mathbf{R}_i)$	$uV_{sp\sigma}$
$E(p_x,p_x,\mathbf{R}_i)$	$u^2V_{pp\sigma} + (1-u^2)V_{pp\pi}$
$E(p_x,p_y,\mathbf{R}_i)$	$uv(V_{pp\sigma} - V_{pp\pi})$

is more than one atom in the basis, the matrices have to be adapted accordingly.

The term H^{SOC} in Eq. (1) is the atomic spin-orbit interaction (see, e.g., Ref. 2),

$$H^{\mathrm{SOC}} = \alpha\mathbf{L}\cdot\mathbf{S} = \alpha\left[\frac{1}{2}(L_-S_+ + L_+S_-) + L_zS_z\right]$$
$$= \alpha/2\begin{pmatrix} 0 & -i & 0 & 0 & 0 & 1 \\ i & 0 & 0 & 0 & 0 & -i \\ 0 & 0 & 0 & -1 & i & 0 \\ 0 & 0 & -1 & 0 & i & 0 \\ 0 & 0 & -i & -i & 0 & 0 \\ 1 & i & 0 & 0 & 0 & 0 \end{pmatrix}. \quad (3)$$

Here the basis of the matrix is $\{p_{x\uparrow}, p_{y\uparrow}, p_{z\uparrow}, p_{x\downarrow}, p_{y\downarrow}, p_{z\downarrow}\}$. The parameter α is the atomic spin-orbit coupling strength.

The third contribution H^z in Eq. (1) takes into account the potential gradient ξ in the z direction perpendicular to the 2D electronic structure, which resides in the xy plane:

$$H^z = \xi z.$$

In order to adapt the Hamiltonian H^z to the tight-binding framework, we divide the contributions from the Hamiltonian H^z into an on-site part $H^{\mathrm{z,onsite}}$ as well as a part coming from neighboring atoms $H^{\mathrm{z,neigh}}$.

In order to calculate the full integral, we use spherical harmonics for the angular part of the wave function. The radial part is approximated by the asymptotic radial wave function R_a as outlined by Slater in Ref. 11:

$$R_a(n^*, Z-s, r) \propto p_{nl}\left(\frac{r}{a_0}\right)^{n^*-1} e^{-[(Z-s)/n^*](r/a_0)}. \quad (4)$$

Here n^* is an effective principal quantum number, Z is the atomic number, s is a screening charge, and $a_0 = 0.529$ Å is the Bohr radius (for details see Ref. 11). Further, we introduce a sign parameter $p_{nl} = (-1)^{n-l-1}$ to ensure an asymptotic approach to zero from positive or negative values. Here, n and l are the principal and orbital quantum numbers, respectively. This asymptotic wave function R_a gives a reasonable approximation for the general behavior of the different tight-binding parameters that will be discussed in the following.

III. ON-SITE CONTRIBUTION FROM H^z

The matrix elements for the on-site Hamiltonian $H^{\mathrm{z,onsite}}$ can be written as

$$H^{\mathrm{z,onsite}}_{oo'} = \langle o|\xi z|o'\rangle = \xi\langle o|r\cos\theta|o'\rangle. \quad (5)$$

Here, r is the radial component in spherical coordinates and $z = r\cos\theta = 2\sqrt{\frac{\pi}{3}}rY_1^0(\theta,\phi)$ represents the conversion from Cartesian to spherical coordinates and to spherical harmonics, respectively. The last step allows us to express the angular part of the integral in Eq. (5) in terms of Gaunt coefficients.[12] From the properties of the Gaunt coefficients, we can directly deduce that the matrix elements in H^z are only nonzero, if $\Delta l = \pm 1$ and $\Delta m = 0$. Furthermore, as the orbitals with $m \neq 0$ are a linear combination of the spherical harmonics, some matrix elements even cancel to zero for $\Delta m = 0$. According to these selection rules the only nonzero elements are sp_z, p_xd_{zx}, p_yd_{yz}, and $p_zd_{z^2}$.

In order to account for the effects of the potential gradient on the on-site sp_z contribution, we define a parameter γ_{sp} in analogy to Ref. 2. Using Eq. (4), we find

$$\gamma_{sp} = \langle s|z|p_z\rangle = -a_0\frac{n^*(1+2n^*)}{2\sqrt{3}(Z-s)}. \quad (6)$$

It serves as an empirical parameter similar to the tight-binding parameters, e.g., $V_{sp\sigma}$. The parameter γ_{sp} depends on the effective principal quantum number n^* through the radial part of the wave function, which defines the spatial extent of the orbital. The parameter γ_{sp} is shown in Fig. 1 as a function of the principal quantum number n. The modulus for γ_{sp} continuously increases with the effective principal quantum number n^*, i.e., the parameter becomes more important for heavier atoms. The increase with n^* can be understood by the increasing spatial extension of the wave function, so that it becomes more sensitive to the effects of the potential gradient. The modulus of γ_{sp} is closely related to the position of the principal maximum $r_{\max} = a_0n^{*2}/(Z-s)$ of the radial charge density $\rho_r \propto r^2R_a^2$.[11]

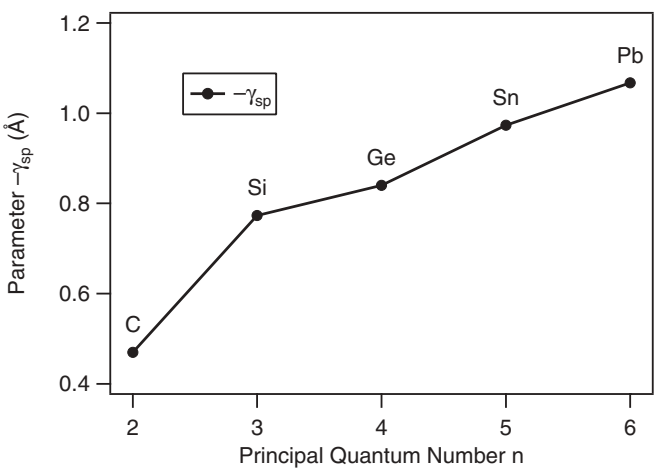

FIG. 1. Overlap integral $-\gamma_{sp}$ as a function of principal quantum number n and for the elements of the fourth group.

IV. NEAREST-NEIGHBOR CONTRIBUTION FROM H^z

The matrix elements for the $H^{\text{z,neigh}}$ Hamiltonian between two neighboring atoms are

$$H^{\text{z,neigh}}_{oo'} = \sum_{\langle i \rangle} e^{i\mathbf{k}\mathbf{R}_i} \langle o|\xi z|o',\mathbf{R}_i\rangle = \sum_{\langle i \rangle} e^{i\mathbf{k}\mathbf{R}_i} \xi \langle o|r\cos\theta|o',\mathbf{R}_i\rangle. \quad (7)$$

These integrals can only be evaluated numerically even for the rather simple wave function of the hydrogen atom. Nevertheless, we can identify the nonzero matrix elements in $H^{\text{z,neigh}}$ and find their angular dependence in terms of the directional cosines. The resulting tight-binding matrix for the contribution of the neighboring atoms to the potential gradient in the basis $\{s, p_x, p_y, p_z\}$ is

$$H^{\text{z,neigh}} = \sum_{\langle i \rangle} e^{i\mathbf{k}\mathbf{R}_i} \xi \begin{pmatrix} 0 & uw(\gamma_{sp2}-\gamma_{sp1}) & vw(\gamma_{sp2}-\gamma_{sp1}) & (1-w^2)\gamma_{sp1}+w^2\gamma_{sp2} \\ uw(\gamma_{sp2}-\gamma_{sp1}) & 0 & 0 & u\gamma_{pp1} \\ vw(\gamma_{sp2}-\gamma_{sp1}) & 0 & 0 & v\gamma_{pp1} \\ (1-w^2)\gamma_{sp1}+w^2\gamma_{sp2} & -u\gamma_{pp1} & -v\gamma_{pp1} & 0 \end{pmatrix}. \quad (8)$$

The quantities u, v, and w, which depend on the vector $\mathbf{R}_i$ connecting two neighboring atoms, are the directional cosines in the x, y, and z direction, respectively. The parameters γ_{sp1}, γ_{sp2}, and γ_{pp1} are defined as

$$\gamma_{sp1} = \langle s|z|p_z, d\mathbf{e}_x\rangle, \quad \gamma_{sp2} = \left\langle s, -\frac{d}{2}\mathbf{e}_z \middle| z \middle| p_z, \frac{d}{2}\mathbf{e}_z \right\rangle, \quad \gamma_{pp1} = \langle p_x|z|p_z, d\mathbf{e}_x\rangle, \quad (9)$$

where d is the nearest-neighbor distance and $\mathbf{e}_i$ are the unit vectors in the respective directions. A matrix element in $H^{\text{z,neigh}}$ will transform even (odd) under exchange of indices if the orbitals have different (same) parity, i.e., $E_\gamma(o',o,-\mathbf{R}_i) = (-1)^{|l-l'+1|} E_\gamma(o,o',\mathbf{R}_i)$. The parameter γ_{sp2} accounts for the nearest-neighbor displacement perpendicular to the xy plane. To calculate γ_{sp2}, the xy plane ($z = 0$) has been set at an equal distance between the neighboring atoms for the influence of the potential on the two neighboring atoms to be equal. Equation (8) applies to the general case of a corrugated 2D system where the vectors connecting the atoms have a z component. If the 2D system is completely flat, then $w \to 0$ and the matrix in Eq. (8) reduces to

$$H^{\text{z,neigh}} = \sum_{\langle i \rangle} e^{i\mathbf{k}\mathbf{R}_i} \xi \begin{pmatrix} 0 & 0 & 0 & \gamma_{sp1} \\ 0 & 0 & 0 & u\gamma_{pp1} \\ 0 & 0 & 0 & v\gamma_{pp1} \\ \gamma_{sp1} & -u\gamma_{pp1} & -v\gamma_{pp1} & 0 \end{pmatrix}. \quad (10)$$

The matrix in Eq. (10) depends on the parameters γ_{sp1} and γ_{pp1}, which account for a lattice residing in the xy plane. If we further reduce the basis to the p orbitals in the lower matrix of Eq. (7), we recover the parameter γ from the potential gradient that was used by Petersen and Hedegård,[2] i.e., $\gamma = \xi\gamma_{pp1}$. In contrast to the on-site contribution of the potential gradient, where only orbitals with $\Delta l = \pm 1$ couple, the contribution from the neighboring atoms also couples orbitals with $\Delta l = 0$ and $\Delta m \neq 0$.

The parameters γ_{sp1}, γ_{sp2}, and γ_{pp1} all depend on the distance d between the neighboring atoms. In order to plot this distance dependence (Fig. 2) we use the asymptotic radial wave function R_a for the carbon atom. The parameters γ_{sp1} and γ_{sp2} have a maximum at zero distance, which is expected as they are closely related to the only nonzero on-site contribution γ_{sp}. The third parameter γ_{pp1} reaches a maximum for a certain distance d between neighboring atoms indicating optimal overlap. For larger distances all three parameters decrease to zero as the overlap between orbitals diminishes.

V. APPLICATION TO GRAPHENE AT $\overline{\mathbf{K}}$

We apply this model to the honeycomb lattice of graphene. A Rashba-type spin splitting has been discussed extensively in the literature,[3–5,13] but the combined aspects of an on-site as well as a nearest-neighbor contribution to the potential gradient have not been considered so far.

The basis vectors $\mathbf{a}_1$ and $\mathbf{a}_2$ as well as the vector τ connecting the two basis atoms (A and B) can be defined using the nearest-neighbor distance d:

$$\mathbf{a}_1 = \frac{d}{2}\begin{pmatrix} -\sqrt{3} \\ 3 \end{pmatrix}, \quad \mathbf{a}_2 = \frac{d}{2}\begin{pmatrix} \sqrt{3} \\ 3 \end{pmatrix}, \quad \tau = d\begin{pmatrix} 0 \\ 1 \end{pmatrix}. \quad (11)$$

With s and p orbitals, two basis atoms, and two spin components, the resulting matrix will be a 16×16 matrix. In

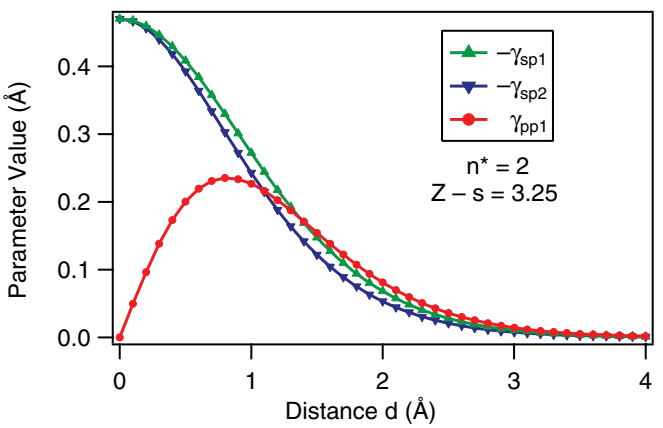

FIG. 2. (Color online) Dependence of the parameters γ_{sp1}, γ_{sp2}, and γ_{pp1} on the distance d between the neighboring atoms. The calculations have been done for the valence orbitals of carbon.

order to compare the results from the Hamiltonian in Eq. (1) to previous results, we project, i.e., downfold, the Hamiltonian in Eq. (1) onto the p_z bands near the $\overline{\mathrm{K}}$ point using a standard theorem:

$$H^{\mathrm{eff}} = PHP + PHQ\frac{1}{\varepsilon - QHQ}QHP. \tag{12}$$

Here, P is a matrix projecting the Hamiltonian near the energy ε onto the p_z orbitals and $Q = 1 - P$. The denominator in the second term of Eq. (12) will be evaluated at the $\overline{\mathrm{K}}$ point with $\alpha = 0$ and $\xi = 0$. The elements of the resulting 4×4 matrix

$$H^{\mathrm{eff}} = \begin{pmatrix} H_{11} & H_{12} & H_{13} & H_{14} \\ H_{12}^* & H_{22} & H_{23} & H_{13} \\ H_{13}^* & H_{23}^* & H_{22} & H_{12} \\ H_{14}^* & H_{13}^* & H_{12}^* & H_{11} \end{pmatrix}, \tag{13}$$

with the basis $\{p_{z\uparrow \mathrm{A}}, p_{z\uparrow \mathrm{B}}, p_{z\downarrow \mathrm{A}}, p_{z\downarrow \mathrm{B}}\}$, are to second order in momentum $\mathbf{k}$:

$$\begin{aligned}
H_{11} &= -d^2\left(k_x^2 + k_y^2\right)\xi^2\frac{\gamma_{\mathrm{pp1}}(V_{\mathrm{sp}\sigma}\gamma_{\mathrm{sp}} + \gamma_{\mathrm{pp1}}\epsilon_s)}{2V_{\mathrm{sp}\sigma}^2} + \xi^2\frac{\gamma_{\mathrm{pp1}}(2V_{\mathrm{sp}\sigma}\gamma_{\mathrm{sp}} + \gamma_{\mathrm{pp1}}\epsilon_s)}{V_{\mathrm{sp}\sigma}^2}, \\
H_{12} &= \frac{3}{2}d(k_x - ik_y)\left(V_{\mathrm{pp}\pi} + \xi^2\frac{2\gamma_{\mathrm{pp1}}\gamma_{\mathrm{sp1}}}{V_{\mathrm{sp}\sigma}}\right) + \frac{3}{8}d^2(k_x + ik_y)^2\left[V_{\mathrm{pp}\pi} - 2\xi^2\gamma_{\mathrm{pp1}}\left(\frac{\gamma_{\mathrm{pp1}}}{V_{\mathrm{pp}\pi} - V_{\mathrm{pp}\sigma}} - \frac{\gamma_{\mathrm{sp1}}}{V_{\mathrm{sp}\sigma}}\right)\right], \\
H_{13} &= -id^2(k_x + ik_y)^2\frac{\alpha\xi}{8}\left(\frac{\gamma_{\mathrm{pp1}}}{V_{\mathrm{pp}\pi} - V_{\mathrm{pp}\sigma}} + \frac{\gamma_{\mathrm{sp1}}}{V_{\mathrm{sp}\sigma}}\right) + d(ik_x + k_y)\frac{\alpha\xi}{2}\left(\frac{\gamma_{\mathrm{pp1}}}{V_{\mathrm{pp}\pi} - V_{\mathrm{pp}\sigma}} - \frac{\gamma_{\mathrm{sp1}}}{V_{\mathrm{sp}\sigma}}\right), \\
H_{14} &= 0, \\
H_{22} &= -d^2\left(k_x^2 + k_y^2\right)\xi^2\frac{\gamma_{\mathrm{pp1}}(V_{\mathrm{sp}\sigma}\gamma_{\mathrm{sp}} + \gamma_{\mathrm{pp1}}\epsilon_s)}{2V_{\mathrm{sp}\sigma}^2} + \frac{18V_{\mathrm{sp}\sigma}\xi^2\gamma_{\mathrm{pp1}}\gamma_{\mathrm{sp}} + \left(\alpha^2 + 9\xi^2\gamma_{\mathrm{pp1}}^2\right)\epsilon_s}{9V_{\mathrm{sp}\sigma}^2}, \\
H_{23} &= id^2\left(k_x^2 + k_y^2\right)\frac{\alpha\xi\gamma_{\mathrm{pp1}}\epsilon_s}{6V_{\mathrm{sp}\sigma}^2} - 2i\frac{\alpha\xi(V_{\mathrm{sp}\sigma}\gamma_{\mathrm{sp}} + \gamma_{\mathrm{pp1}}\epsilon_s)}{3V_{\mathrm{sp}\sigma}^2}.
\end{aligned} \tag{14}$$

In order to better understand the origin of the different terms in Eq. (14) and their effect on the band dispersion, we compare the matrix elements in Eq. (14) to the Hamiltonian expressed in terms of the basis functions of the trigonal graphene band structure near the $\overline{\mathrm{K}}$ point from Ref. 14:

$$\begin{aligned}
H^{\mathrm{sym}} = {} & a_{10} + a_{61}(k_x\sigma_x + k_y\sigma_y) + a_{11}\left(k_x^2 + k_y^2\right) + a_{62}\left[\left(k_y^2 - k_x^2\right)\sigma_x + 2k_xk_y\sigma_y\right] + \alpha\, p_{21}s_z\sigma_z + \alpha\, p_{22}\left(k_x^2 + k_y^2\right)s_z\sigma_z \\
& + \xi\, r_{62}(s_y\sigma_x - s_x\sigma_y) + \xi\, r_{11}(k_xs_y - k_ys_x) + \xi\, r_{64}[(k_xs_x - k_ys_y)\sigma_y + (k_ys_x + k_xs_y)\sigma_x] \\
& + \xi\, r_{12}\left[\left(k_x^2 - k_y^2\right)s_x - 2k_xk_ys_y\right] + \xi\, r_{63}\left[2k_xk_ys_x\sigma_x - \left(k_x^2 - k_y^2\right)s_y\sigma_x - 2k_xk_ys_y\sigma_y + \left(k_y^2 - k_x^2\right)s_x\sigma_y\right] \\
& + \xi\, r_{65}\left(k_x^2 + k_y^2\right)(s_y\sigma_x - s_x\sigma_y).
\end{aligned} \tag{15}$$

For brevity, the superscripts of the coefficients in Ref. 14 as well as the unit matrices have been omitted. The s_i and σ_i $(i = x,y,z)$ are the Pauli-spin and pseudospin matrices, respectively. The coefficients a_{ij}, p_{ij}, and r_{ij} refer to the intrinsic band dispersion, the spin-orbit coupling α, and the effects of an external electric field ξ along the z direction, respectively. We find a direct correspondence between the Hamiltonian H^{eff} and H^{sym}:

$$\begin{aligned}
a_{10} &= \frac{2\xi^2\gamma_{\mathrm{pp1}}\gamma_{\mathrm{sp}}}{V_{\mathrm{sp}\sigma}} + \frac{\left(\alpha^2 + 18\xi^2\gamma_{\mathrm{pp1}}^2\right)\epsilon_s}{18V_{\mathrm{sp}\sigma}^2}, \\
a_{11} &= -\frac{d^2\xi^2\gamma_{\mathrm{pp1}}(V_{\mathrm{sp}\sigma}\gamma_{\mathrm{sp}} + \gamma_{\mathrm{pp1}}\epsilon_s)}{2V_{\mathrm{sp}\sigma}^2}, \\
a_{61} &= \frac{3}{2}d\left(V_{\mathrm{pp}\pi} + \frac{2\xi^2\gamma_{\mathrm{pp1}}\gamma_{\mathrm{sp1}}}{V_{\mathrm{sp}\sigma}}\right), \\
a_{62} &= -\frac{3}{8}d^2\left[V_{\mathrm{pp}\pi} - 2\xi^2\gamma_{\mathrm{pp1}}\left(\frac{\gamma_{\mathrm{pp1}}}{V_{\mathrm{pp}\pi} - V_{\mathrm{pp}\sigma}} - \frac{\gamma_{\mathrm{sp1}}}{V_{\mathrm{sp}\sigma}}\right)\right], \\
p_{21} &= -\frac{\alpha\epsilon_s}{18V_{\mathrm{sp}\sigma}^2}, \\
p_{22} &= 0, \\
r_{11} &= -d\frac{\alpha}{2}\left(\frac{\gamma_{\mathrm{pp1}}}{V_{\mathrm{pp}\pi} - V_{\mathrm{pp}\sigma}} - \frac{\gamma_{\mathrm{sp1}}}{V_{\mathrm{sp}\sigma}}\right), \\
r_{12} &= -id^2\frac{\alpha}{8}\left(\frac{\gamma_{\mathrm{pp1}}}{V_{\mathrm{pp}\pi} - V_{\mathrm{pp}\sigma}} + \frac{\gamma_{\mathrm{sp1}}}{V_{\mathrm{sp}\sigma}}\right), \\
r_{62} &= \alpha\left(\frac{\gamma_{\mathrm{sp}}}{3V_{\mathrm{sp}\sigma}} + \frac{\gamma_{\mathrm{pp1}}\epsilon_s}{3V_{\mathrm{sp}\sigma}^2}\right), \\
r_{64} &= 0, \\
r_{63} &= 0, \\
r_{65} &= -d^2\alpha\frac{\gamma_{\mathrm{pp1}}\epsilon_s}{12V_{\mathrm{sp}\sigma}^2}.
\end{aligned} \tag{16}$$

All terms in Eq. (16) are influenced by the electric field ξ (through the parameters $\gamma_{oo'x}$) and/or the atomic spin-orbit coupling strength α to second order, i.e., α^2, $\alpha\xi$, or ξ^2. The coefficients for the unperturbed band dispersion a_{ij} are corrected by terms proportional to ξ^2 and/or α^2 from the nearest-neighbor contributions to the Hamiltonian H^z. Terms to second order in ξ and α have not explicitly been considered in the expansion of the basis functions in Ref. 14. They result

from the projection of the Hamiltonian [Eq. (1)] and are thus included for completeness. This affects the value of the band velocity $\hbar v_F$ related to a_{61} as well as second-order corrections to the linear band dispersion from the coefficients a_{11} and a_{62}. The coefficient a_{10} is a constant offset corresponding to a rigid-band shift, which has no further consequence for the subsequent discussion. For the coefficients associated with the spin-orbit interaction p_{ij}, the present tight-binding model contributes only to second order in the atomic spin-orbit coupling strength α via the parameter p_{21}. This result has been obtained previously.[5]

The coefficients r_{ij} are related to the first-order contribution of the electric field ξ. They also depend linearly on the spin-orbit coupling α. The coefficient r_{62} can be identified with the zeroth-order Rashba constant λ_R (see, e.g., Refs. 4 and 5). Aside from the first term in r_{62}, which originates from the on-site contribution in H^z, all other contributions to r_{ij} come from the nearest-neighbor contribution. The on-site contribution in r_{62} has been considered in previous models[4,5] and can be constructed from the effective on-site Rashba term:[6]

$$H^{\mathrm{R,onsite}} = V_R(s_y\sigma_x - s_x\sigma_y), \tag{17}$$

where V_R is the corresponding effective coupling constant, with $V_R = \alpha\xi\frac{\gamma_{sp}}{3V_{sp\sigma}}$. The second term in r_{62} has not been considered in previous models.[4,5] It is of the same order of magnitude as the first (on-site) term, but originates from the nearest-neighbor contribution in H^z. It can be constructed from the effective nearest-neighbor Rashba term to zeroth order in momentum $\mathbf{k}$, which has been discussed in Ref. 6 and in more detail in Ref. 14:

$$H^{\mathrm{R,neigh}} = \begin{pmatrix} 0 & h_R \\ h_R^* & 0 \end{pmatrix};\quad h_R = V_R' \sum_{\langle i\rangle} i e^{i\mathbf{k}\mathbf{R}_i}\left(\mathbf{s}\times\frac{\mathbf{R}_i}{|\mathbf{R}_i|}\right)\cdot\hat{z}, \tag{18}$$

where the sum is over nearest neighbors, V_R' is the corresponding effective coupling constant, $\hat{z}$ is the unit vector in the z direction, and $\mathbf{s}$ is the vector of Pauli matrices.[6,14] The second term in r_{62} opens up a new path in the effective nearest-neighbor hopping of two p_z orbitals in addition to the one discussed in Ref. 4. This means that the effect of the electric field ξ on the spin-splitting in graphene is larger than previously assumed. Further, the effective nearest-neighbor Rashba term in Eq. (18) has nonzero coefficients, which are zero in the tight-binding model (r_{63} and r_{64}). The coefficients extracted from Eq. (18) are up to second order in momentum $\mathbf{k}$:

$$\begin{aligned} \xi r_{62} &= \tfrac{3}{2}V_R', \\ \xi r_{64} &= \tfrac{3}{4}dV_R', \\ \xi r_{63} &= \tfrac{3}{16}d^2V_R', \\ \xi r_{65} &= -\tfrac{3}{8}d^2V_R'. \end{aligned} \tag{19}$$

Here, $V_R' = \alpha\xi\frac{2\gamma_{pp1}\epsilon_s}{9V_{sp\sigma}^2}$ when comparing the coefficients to the tight-binding model. Other contributions not considered in the present tight-binding model (e.g., higher-order orbitals) may result in nonzero coefficients r_{63} and r_{64}. On the other hand, the coefficient r_{11} is nonzero in the tight-binding model, but cannot be constructed from either Eqs. (17) or (18).[14] It can be assigned to the "linear" Rashba constant α_R from the "conventional" Bychkov-Rashba model,[1] as the corresponding basis function shows the same linear momentum dependence. It introduces a spin-dependent correction to the band velocity $\hbar v_F$. The coefficients r_{12} and r_{65} both give a correction to second order in momentum. In this way, the tight-binding model unifies different phenomenological descriptions [Eqs. (17) and (18)] demonstrating that even though they have similar effects on the band dispersion, they actually have a different origin (the on-site and nearest-neighbor contribution, respectively).

In order to make the effects of the different contributions more obvious we reduce the Hamiltonian H^{eff} in Eqs. (13) and (14) to first order in momentum k. This enables us to calculate the energy eigenvalues in an analytical form. We find

$$\begin{aligned} &E_{\mu,\lambda}(\mathbf{k}) \\ &\quad = a_{10} + \lambda\xi r_{62} + \mu\sqrt{\mathbf{k}^2(a_{61}+\lambda\xi r_{11})^2 + (p_{21}-\lambda\xi r_{62})^2}, \end{aligned} \tag{20}$$

where $\mu = \pm 1$ refers to the valence/conduction band and $\lambda = \pm 1$ is the index for the spin eigenstate. The origin of the momentum $\mathbf{k}$ is set at the $\overline{\mathrm{K}}$ point. We can associate the coefficients of the basis functions with the band velocity $\hbar v_F$, the intrinsic spin-orbit splitting Δ_{SO}, as well as the zeroth and first-order Rashba constants λ_R and α_R:

$$\begin{aligned} \hbar v_F &= a_{61} + \lambda\xi\, r_{11} \\ &= \frac{3}{2}d\left(V_{pp\pi} + \xi^2\frac{2\gamma_{pp1}\gamma_{sp1}}{V_{sp\sigma}}\right) \\ &\quad - \lambda d\frac{\alpha\xi}{2}\left(\frac{\gamma_{pp1}}{V_{pp\pi}-V_{pp\sigma}} - \frac{\gamma_{sp1}}{V_{sp\sigma}}\right), \\ \Delta_{\mathrm{SOC}} &= \alpha\, p_{21} = -\frac{\alpha^2\epsilon_s}{18V_{sp\sigma}^2}, \\ \lambda_R &= \xi\, r_{62} = \frac{\alpha\xi\gamma_{sp}}{3V_{sp\sigma}} + \frac{\alpha\xi\gamma_{pp1}\epsilon_s}{3V_{sp\sigma}^2}, \\ \alpha_R &= \xi\, r_{11} = -d\frac{\alpha\xi}{2}\left(\frac{\gamma_{pp1}}{V_{pp\pi}-V_{pp\sigma}} - \frac{\gamma_{sp1}}{V_{sp\sigma}}\right). \end{aligned} \tag{21}$$

For a numerical evaluation of the parameters in Eq. (21), we have to calculate the potential gradient parameters γ_{sp}, γ_{sp1}, and γ_{pp1} using Eqs. (6) and (9). Again, we use the asymptotic radial wave function R_a for the carbon atom. Further, for the atomic spin-orbit coupling strength we assume $\alpha = 8.5$ meV,[15] and for the electric field we estimate $\xi = 0.1\ \frac{\mathrm{eV}}{\mathrm{\AA}}$, which is a reasonable value for a graphene layer on a substrate. With the potential gradient parameters $\gamma_{sp} = -0.47$ Å, $\gamma_{sp1} = -0.16$ Å, and $\gamma_{pp1} = 0.17$ Å, as well as the tight-binding parameters from Table II, we find at the $\overline{\mathrm{K}}$ point

$$\begin{aligned} \hbar v_F &= -6.46\ \mathrm{eV\,\mathring{A}} + \lambda \times 107.7\ \mu\mathrm{eV\,\mathring{A}}, \\ \Delta_{\mathrm{SOC}} &= 1.14\ \mu\mathrm{eV}, \\ \lambda_R &= 37.4\ \mu\mathrm{eV}, \\ \alpha_R &= 6.46\ \mu\mathrm{eV\,\mathring{A}}. \end{aligned} \tag{22}$$

TABLE II. Tight-binding parameters of graphene with a nearest-neighbor distance of $d = 1.42$ Å (Refs. 5 and 16).

Parameter	Value (eV)
ϵ_s	−8.868
ϵ_p	0.000
$V_{ss\sigma}$	−6.769
$V_{sp\sigma}$	5.580
$V_{pp\sigma}$	5.037
$V_{pp\pi}$	−3.033

The band velocity $\hbar v_F$ agrees with experimental values (see, e.g., Ref. 17). The band dispersion near the $\overline{\mathrm{K}}$ point is shown in Fig. 3 for different scenarios. It is clearly visible that the nearest-neighbor parameters γ_{sp1} and γ_{pp1} give a sizable contribution to the spin splitting. Away from the $\overline{\mathrm{K}}$ point, we find for the momentum dependent energy splitting ΔE between the spin-split branches

$$\Delta E = 2\lambda_R + 2\,|\mathbf{k}|\,\alpha_R. \tag{23}$$

Therefore the nearest-neighbor contribution to the Hamiltonian H^z does not only give a correction to the constant spin splitting, but also introduces an additional term, which depends linearly on momentum.

VI. APPLICATION TO $\mathbf{p}_z$ BANDS AT $\overline{\Gamma}$

We have carried out a similar analysis for the p_z bands at the $\overline{\Gamma}$ point, in analogy to the calculation presented for the $\overline{\mathrm{K}}$ point above. In addition to the honeycomb lattice of graphene with two atoms per unit cell, we have also calculated the corresponding Hamiltonians for a hexagonal and a quadratic lattice with one atom per unit cell. As the symmetry at the $\overline{\Gamma}$ point is higher than at the $\overline{\mathrm{K}}$ point, we expect the set of allowed basis functions for the band dispersion to be smaller. The energy dispersion, which we have found from the tight-binding model presented here to second order in momentum $\mathbf{k}$, is

$$E_\lambda(\mathbf{k}) = \frac{\hbar^2}{2m}\mathbf{k}^2 + \lambda\alpha_R\,|\mathbf{k}| + E_0 \tag{24}$$

with the origin of the momentum $\mathbf{k}$ at the $\overline{\Gamma}$ point. The projection given in Eq. (12) has been carried out at $\varepsilon = \eta V_{pp\pi}$ with η being the number of nearest neighbors in the respective lattice. The different coefficients in terms of the tight-binding parameters are

$$\begin{aligned}
\frac{\hbar^2}{2m} &= -\frac{1}{4}d^2\eta\left(V_{pp\pi} - \frac{2\xi^2\gamma_{pp1}^2}{V_{pp\pi}-V_{pp\sigma}} + \frac{2\xi^2\gamma_{sp1}(\gamma_{sp}+\eta\gamma_{sp1})}{\eta V_{pp\pi}-\eta V_{ss\sigma}-\epsilon_s}\right),\\
E_0 &= \eta V_{pp\pi} + \frac{\alpha^2}{\eta V_{pp\pi}-\eta V_{pp\sigma}} + \frac{\xi^2(\gamma_{sp}+\eta\gamma_{sp1})^2}{\eta V_{pp\pi}-\eta V_{ss\sigma}-\epsilon_s},\\
\alpha_R &= \frac{d\alpha\xi\gamma_{pp1}}{V_{pp\pi}-V_{pp\sigma}}.
\end{aligned} \tag{25}$$

Here, d is the nearest-neighbor distance of the respective lattice. Because of the high symmetry at the $\overline{\Gamma}$ point, the zeroth-order Rashba parameter λ_R is zero so that the lowest-order contribution is the linear Rashba constant α_R. It is equivalent to the phenomenological description of the nearest-neighbor Rashba term.[6,8] The results for the different lattices (effective mass and energy offset) only differ from each other by the number of nearest neighbors involved, i.e., $\eta = 3$ for the honeycomb lattice, $\eta = 4$ for the quadratic lattice, and $\eta = 6$ for the hexagonal lattice. A schematic of the band dispersion is shown in Fig. 4. The characteristic offset can be clearly seen. Since $\overline{\Gamma}$ is a time-reversal invariant point in the two-dimensional Brillouin zone, the spin-split band remains degenerate there. The atomic spin-orbit coupling strength α and the electric field ξ introduce small corrections to the

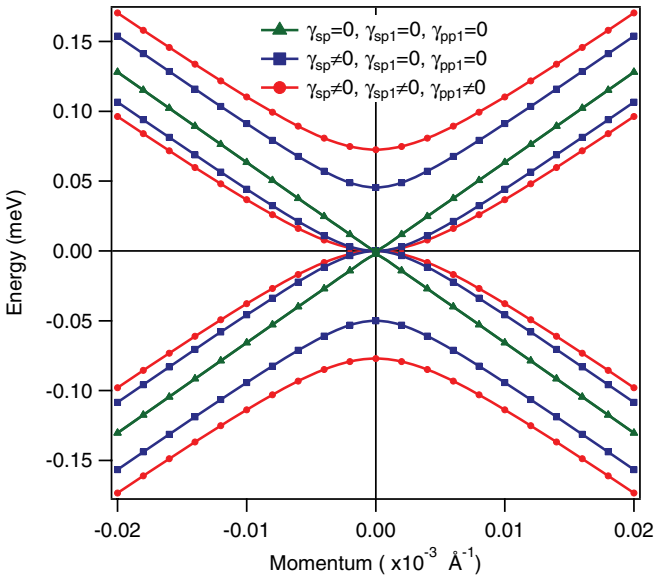

FIG. 3. (Color online) Dispersion of the graphene bands near the Fermi level at the $\overline{\mathrm{K}}$ point for different contributions from the potential gradient.

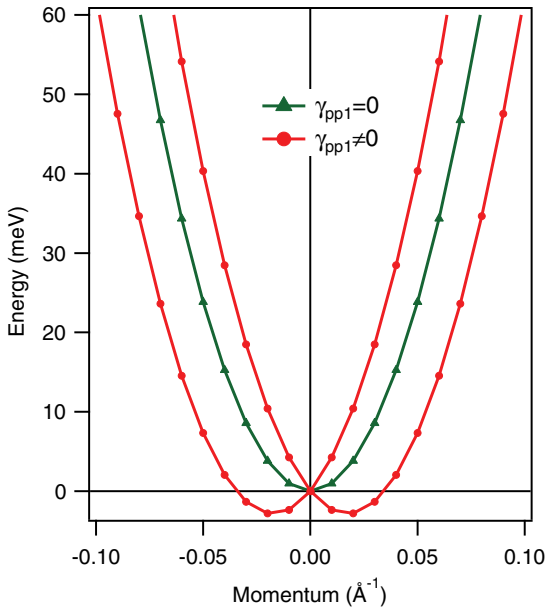

FIG. 4. (Color online) Dispersion of a two-dimensional state at the $\overline{\Gamma}$ point for different contributions from the potential gradient. The effective mass m is 0.4 m_e (m_e: free electron mass), the energy offset E_0 is zero, and the linear Rashba constant α_R is 0.33 eV Å.

effective mass and the energy offset. Interestingly, the linear Rashba constant α_R only depends on the electric field ξ through the nearest-neighbor overlap of the p_{xy} orbitals with the p_z orbital in agreement with Petersen and Hedegård;[2,18] it does not depend on the on-site contribution γ_{sp}. Moreover, the linear Rashba constant α_R is independent of the details in the three lattices. This gives the result a certain kind of universality.

VII. APPLICATION TO A CORRUGATED LATTICE

Many systems with a sizable Rashba-type spin splitting have a corrugated surface structure (e.g., Bi, Sb, Ag, or Cu based surface alloys with Bi, Pb, Sb).[19–25] The simplest approach to describe a corrugated surface is a honeycomb lattice where the two basis atoms are displaced by $\pm\Delta z$ from the xy plane. This structure mimics the topmost surface layer of, e.g., the Bi(111) or Sb(111) surface. The linear Rashba constant α_R in a corrugated honeycomb lattice amounts to

$$\alpha_R = \frac{d\alpha\xi\gamma_{\mathrm{pp1}}}{V_{\mathrm{pp}\pi} - V_{\mathrm{pp}\sigma}} \tag{26}$$

and is identical to the one for the uncorrugated lattice [see Eq. (25)]. It increases proportionally to the nearest-neighbor distance d. As the values of the tight-binding parameters decrease with increasing distance d (see, e.g., Ref. 26), we expect a corresponding increase in the Rashba constant as well.

In the literature, a strong increase of the Rashba-type spin splitting due to the corrugation of the surface has been discussed extensively.[25,27–30] In particular, for the Ag and Cu based surface alloys with Bi, Pb, or Sb, a correspondence between the outward relaxation of the alloy atoms and the strength of the Rashba-type spin splitting has been observed.[29] However, for the tight-binding model presented here a corrugation of the lattice does not result in a particular enhancement of the Rashba-type spin splitting. Obviously, a more detailed model, possibly an inclusion of the d bands[4] or higher-order contributions to the Rashba coefficient,[31] is needed to describe this enhancement by corrugation.

VIII. CONCLUSION

In summary, we have presented an extended sp-band tight-binding model for the Rashba-type spin splitting in two-dimensional lattices by combining the on-site and nearest-neighbor contributions from the potential gradient. Concerning the conical band structure near the $\overline{\mathrm{K}}$ point of graphene, it combines the effective on-site and nearest-neighbor Rashba terms [Eqs. (17) and (18)] along with other Rashba terms that are not included in the effective Rashba terms. The tight-binding model thus further validates the already successful phenomenological description at the same time pointing out that it is not complete. The nearest-neighbor contribution from the potential gradient gives a sizable contribution to the zeroth-order Rashba constant λ_R as well as a nonzero linear Rashba constant α_R. Hence both the on-site and the nearest-neighbor contribution should be considered in model calculations. At the $\overline{\Gamma}$-point quadratic, hexagonal as well as flat and corrugated honeycomb lattices all give the same simple expression for the linear Rashba parameter α_R, which only depends on the nearest-neighbor contribution from the potential gradient. In particular, it is independent of the details of the lattices giving the result a certain kind of universality and confirms the success of the phenomenological nearest-neighbor Rashba term. The next step would be to combine this model with the results from d-band contributions[4] and higher-order contributions to the Rashba coefficient,[31] which have been shown to add to the Rashba-type spin splitting. Successively including more components to this model will at the end lead to a better understanding of the Rashba-type spin splitting at surfaces.

ACKNOWLEDGMENTS

We gratefully acknowledge M. Haverkort, J. Henk, and R. Winkler for valuable discussions. C.R.A. acknowledges funding from the Emmy-Noether Program of the Deutsche Forschungsgemeinschaft (DFG).

*Corresponding author: c.ast@fkf.mpg.de

[1] Yu. A. Bychkov and E. I. Rashba, Pis'ma Zh. Eksp. Teor. Fiz. **39**, 66 (1984) [JETP Lett. **39**, 78 (1984)].
[2] L. Petersen and P. Hedegård, Surf. Sci. **459**, 49 (2000).
[3] D. Huertas-Hernando, F. Guinea, and A. Brataas, Phys. Rev. B **74**, 155426 (2006).
[4] S. Konschuh, M. Gmitra, and J. Fabian, Phys. Rev. B **82**, 245412 (2010).
[5] H. Min, J. E. Hill, N. A. Sinitsyn, B. R. Sahu, L. Kleinman, and A. H. MacDonald, Phys. Rev. B **74**, 165310 (2006).
[6] C. L. Kane and E. J. Mele, Phys. Rev. Lett. **95**, 226801 (2005).
[7] M. H. Liu and C. R. Chang, Phys. Rev. B **80**, 241304 (2009).
[8] M. H. Liu, S. H. Chen, and C. R. Chang, Phys. Rev. B **78**, 195413 (2008).
[9] L. Sheng, D. N. Sheng, C. S. Ting, and F. D. M. Haldane, Phys. Rev. Lett. **95**, 136602 (2005).
[10] J. C. Slater and G. F. Koster, Phys. Rev. **94**, 1498 (1954).
[11] J. C. Slater, Phys. Rev. **36**, 57 (1930).
[12] J. A. Gaunt, Philos. Trans. R. Soc. London A **228**, 151 (1929).
[13] S. Abdelouahed, A. Ernst, J. Henk, I. V. Maznichenko, and I. Mertig, Phys. Rev. B **82**, 125424 (2010).
[14] R. Winkler and U. Zülicke, Phys. Rev. B **82**, 245313 (2010).
[15] F. Kuemmeth, S. Ilani, D. C. Ralph, and P. L. McEuen, Nature (London) **452**, 448 (2008).
[16] R. Saito, M. Fujita, G. Dresselhaus, and M. S. Dresselhaus, Phys. Rev. B **46**, 1804 (1992).
[17] A. Bostwick, T. Ohta, T. Seyller, K. Horn, and E. Rotenberg, Nat. Phys. **3**, 36 (2007).
[18] In Ref. 2, the authors present an expression for the linear Rashba constant α_R, which is slightly different from ours. We trace this back to a calculational error on their part. Furthermore, the nearest-neighbor distance d does not enter in their calculation. Nevertheless, we believe that the main conclusions that can be drawn are the same.

[19]C. R. Ast and H. Höchst, Phys. Rev. Lett. **87**, 177602 (2001).
[20]Y. M. Koroteev, G. Bihlmayer, J. E. Gayone, E. V. Chulkov, S. Blügel, P. M. Echenique, and P. Hofmann, Phys. Rev. Lett. **93**, 046403 (2004).
[21]L. Moreschini, A. Bendounan, H. Bentmann, M. Assig, K. Kern, F. Reinert, J. Henk, C. R. Ast, and M. Grioni, Phys. Rev. B **80**, 035438 (2009).
[22]L. Moreschini, A. Bendounan, I. Gierz, C. R. Ast, H. Mirhosseini, H. Höchst, K. Kern, J. Henk, A. Ernst, S. Ostanin *et al.*, Phys. Rev. B **79**, 075424 (2009).
[23]D. Pacilé, C. R. Ast, M. Papagno, C. DaSilva, L. Moreschini, M. Falub, A. P. Seitsonen, and M. Grioni, Phys. Rev. B **73**, 245429 (2006).
[24]K. Sugawara, T. Sato, S. Souma, T. Takahashi, M. Arai, and T. Sasaki, Phys. Rev. Lett. **96**, 046411 (2006).
[25]C. R. Ast, J. Henk, A. Ernst, L. Moreschini, M. C. Falub, D. Pacilé, P. Bruno, K. Kern, and M. Grioni, Phys. Rev. Lett. **98**, 186807 (2007).
[26]W. A. Harrison, *Electronic Structure and the Properties of Solids: The Physics of the Chemical Bond* (Freeman, San Francisco, 1980).
[27]G. Bihlmayer, S. Blügel, and E. V. Chulkov, Phys. Rev. B **75**, 195414 (2007).
[28]J. H. Dil, J. Phys.: Condens. Matter **21**, 403001 (2009).
[29]I. Gierz, B. Stadtmüller, J. Vuorinen, M. Lindroos, F. Meier, J. H. Dil, K. Kern, and C. R. Ast, Phys. Rev. B **81**, 245430 (2010).
[30]J. Henk, A. Ernst, and P. Bruno, Surf. Sci. **566–568**, 482 (2004).
[31]S. Vajna, E. Simon, A. Szilva, K. Palotas, B. Ujfalussy, and L. Szunyogh, Phys. Rev. B **85**, 075404 (2012).